We are IntechOpen, the world's leading publisher of Open Access books Built by scientists, for scientists

6,900
Open access books available

186,000
International authors and editors

200M
Downloads

Our authors are among the

154
Countries delivered to

TOP 1%
most cited scientists

12.2%
Contributors from top 500 universities

CLARIVATE ANALYTICS
BOOK CITATION INDEX
INDEXED

WEB OF SCIENCE™

Selection of our books indexed in the Book Citation Index
in Web of Science™ Core Collection (BKCI)

Interested in publishing with us?
Contact book.department@intechopen.com

Numbers displayed above are based on latest data collected.
For more information visit www.intechopen.com

Evolution of Cosmic System

Noboru Tanizuka

Additional information is available at the end of the chapter

http://dx.doi.org/10.5772/51435

1. Introduction

What does it mean that the cosmic radio wave flux density varies with the passage of time is an interesting question; the radio wave is of the quasar, a system of galaxy, which is distributed in our universe from a few billions of light years to the distanse close to the big bang age and has been radiating immense electromagnetic energy from it by the synchrotron radiation that we may able to make a measurement of the flux density at micro wave bands with a radio interferometer[3,4]. A group of radio observers and astronomers has been monitoring daily so far over several years extragalactic radio sources (radio galaxies, quasars, etc.) and the monitored data were kindly shared with us who were interested in using for analysis[5]. In a few recent decades, the chaos and fractal theory has been intensively studied and developed in the fields of mathematics, computer numerical analysis, natural sciences and technologies[1], and in same decades, the nonlinear time series analysis methods have been developed intensely based on the newly understood ideas of the theory for analyzing the nonlinear phenonena[2].

The study in this chapter is motivated by the three factors mentioned above to analyze the time series of the radio wave flux density from the cosmological object, primarily, with one of the nonlinear methods, for finding the dynamics related to the cosmic object, including its information in the flux density variations. We hoped that if we could infer the dynamics and if the result would be found to have any rule changing with the magnitude of the red shift of the object we might have some knowledge concerning to the evolution of our universe. The hope has been prompted us to continue consistently to analyze the time series data. The period of monitor over several years is extremely short compared with the cosmic age, however , the analysis result of the time series data in newly developing methods may give us a new sight viewed from the nonlinear dynamics in the short time scale for the cosmic dynamical system.

2. Linear and nonlinear systems

2.1. Linear system

The result of a linear data computed with Fourier spectral analysis gives a pure periodicity, which means predictability of event(s) for unlimited future. No event of evolution can be expected by a linear data, and a linear system is not a way of our natural world. On the other hand, the result of a pure random data computed with it gives no structure of the periodicity, a continuous spectrum, and means no event of predictability.

2.2. Nonlinear system

One of discrete nonlinear dynamical systems is given in this section for explanation. The logistic map function is given in Eq.(1) with a difference equation. Given that the time series data is generated from this system by iterating at $t = 0, 1, .., N$.

$$f(x) = ax(1 - x); \; x(t + 1) = f(x(t)) \tag{1}$$

The result of the Fourier analysis for the time series data at parameter $a = 4.0$ in the function of Eq.(1) is indistinguishable from the result of the random data. The spectra for the random data and logistic time series data are given in Fig.1. The latter comes from the deterministic system, but the analysis result does not disclose the nonlinearity of the data. This is a reason why a help of a new method is necessary for the analysis of data from the natural phenomena which are often complex for us to understand and may include such complexity as above in part. A method to distinguish between the kinds of data is to draw a graph composed of coordinates with time-lagged components, that is, a graphical execution of differentiation for a time series. The result of the graphical execution for the random and logistic time series in Fig. 1 is shown in Fig. 2. As a result, in the figure the two time series are correctly discriminated. The time series generated from Eq.(1) resulted in a quadratic expression with the second dimension of coordinates (see Fig. 2(b)). On the other hand, the random time series resulted in the uncorrelated graph as shown in Fig. 2(a).[1]

The time series data measured from natural and social systems is not generated in such a mathematical way and so complicated that more intricated process is required to deal with data. This problem will be discussed in later sections. Before we do this, some methods of quantifying fractal data and some characteristics of chaos dynamics (the initial value dependence and the parametric dependence) are exemplified by the logistic system.

Time series data were generated from Eq.(1) at parameter $a = 3.7$ with two initial values at $x(0) = 0.10000$ and at $x(0) = 0.10001$, and the two time series are drawn as the diagram shown in Fig. 3 (left). The diagram shows that the trajectories of the two time series separate in a few tens of iteration time, which means that a small error was extended to a magnitude of space the time series occupies within the limited time and the prediction is failed over the

---

[1] It is true in the second dimension of coordinates. If the time series is generated by the function of higher degree, the correlation may be true in the graph at a higher dimension of coordinates.
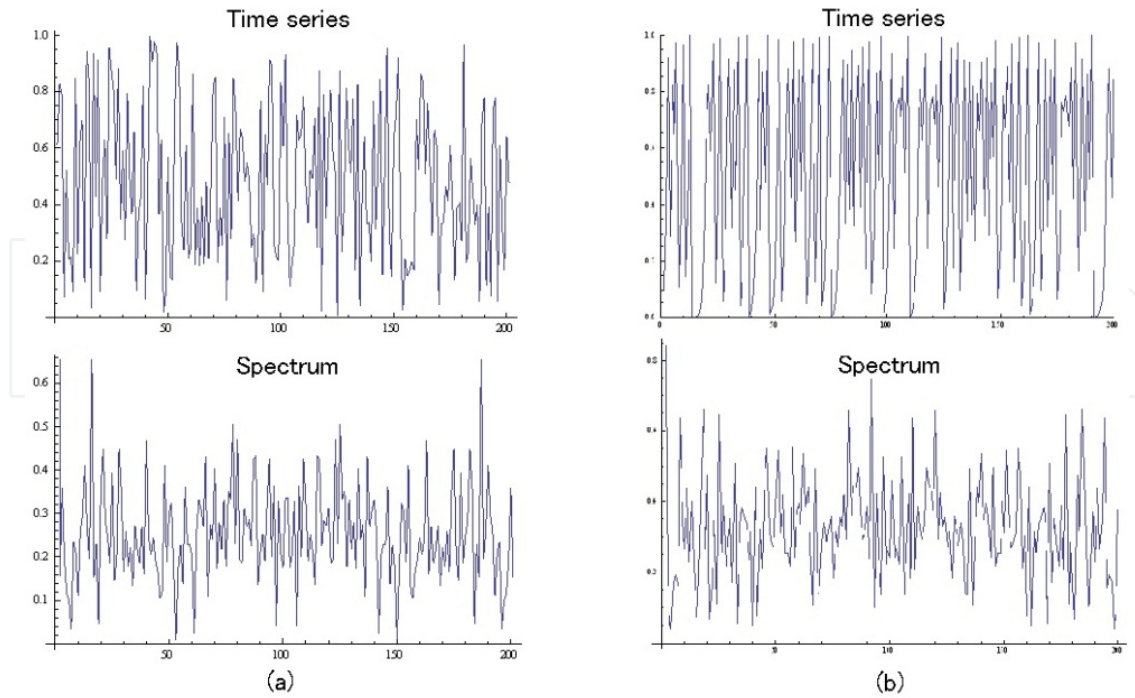
Figure 1. Fourier analysis for time series data of (a) uniform random numbers and (b) logistic map system at $a = 4.0$. The spectrum is shown by the absolute of the Fourier transform.
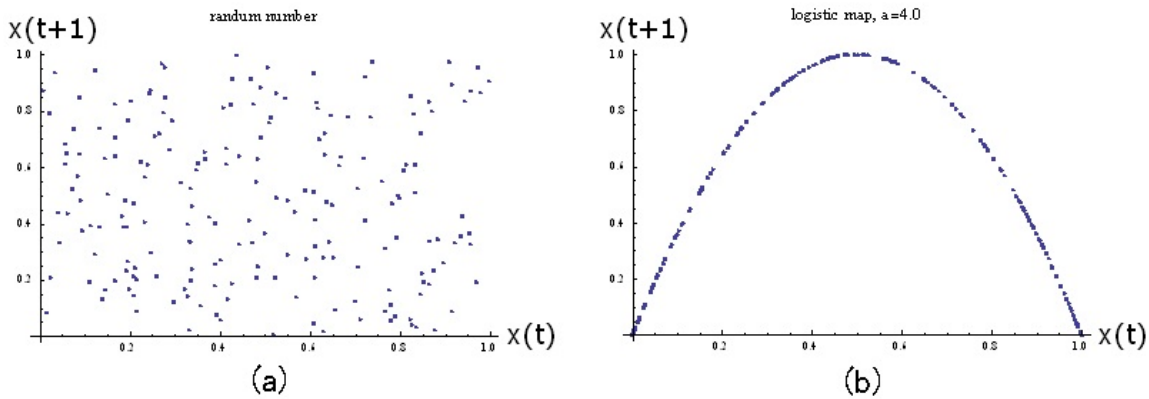

Figure 2. Graphical analysis for (a) random time series data and (b) logistic time series data given in Fig. 1.

time. This means that in spite of extremely small error in the chaos deterministic system, the error is extended to a scale of state space in a limited time, that the system is unpredictable. The fact was explained in the Fourier spectrum of the time series in Fig. 1 (b).

The parametric dependence is characteristic to a chaos system. The vertical axis on the right diagram in Fig. 3 shows the values of number computed by Eq.(1) at parameter a in the range of $3.8 \leq a \leq 4.0$, along the horizontal axis. At a parameter value between 3.82 and 3.83, the behavior of the system drastically changes to periodicity. In the logistic system the parameter is interpreted as the environment for a living thing to survive. For nonlinear systems, a parameter value becomes crucial for the system's behavior. For example, in the logistic dynamics, extinction or evolution of the system depends on the parameter value.
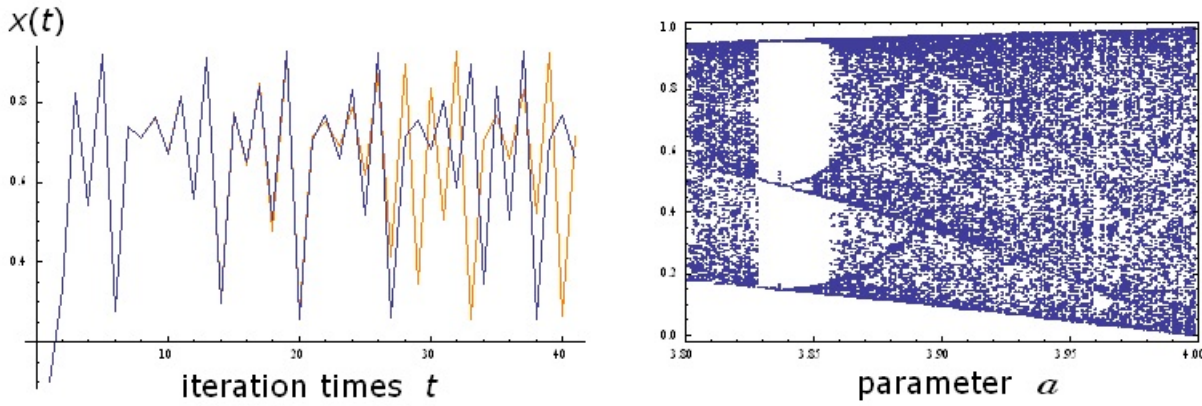
Figure 3. Logistic time series at parameter $a = 3.7$ and at initial values $x(0) = 0.10000$ and $x(0) = 0.10001$ (orange) on the left, and the bifurcation diagram in the parameter range over $3.8 \leq a \leq 4.0$ on the right.

3. Quantitative properties of nonlinearity

Time series data of a natural system may often be of a nonlinear dynamics, about which we know little for the system and need to analyze in an appropreate method in assumed state space dimensions. In this section we discuss on the way how to quantify such data assumed to be nonlinear by exemplifying the analysis for the logistic system.

3.1. Lyapunov exponent and information entropy

The initial value dependence of a system is evaluated by the Lyapunov exponent given by

$$\lambda = \lim_{N \to \infty} \frac{1}{N} \sum_{t=0}^{N-1} \log|f'(x(t))| , \qquad (2)$$

for the discrete system, and $\lambda = \lim_{t \to \infty} t^{-1} \log d_t/d_0$ for the continuous system with d_0, d_t the initial error and its expansion at time t, respectively. It is easy to understand that if the system is in the chaos, $\lambda > 0$, the error is exponentially extended. Even if we have this way to distinguish a system whether it is a chaos system or a mere random system, it is a difficult problem to analyze λ of a time series data because the system's function f is not in our hand.

The information entropy of a system, as its manifold is given in a state space, is defined as

$$H(\varepsilon) = -\sum_{i=1}^{M} p_i \log p_i, \quad \sum_{i=1}^{M} p_i = 1 , \qquad (3)$$

where ε is an infinitesimal length with a super cube and M the number of cubes with which cover whole manifold in the state space. Equation (3) quantifies the distribution of data points in the state space as the average number of the amount of information.

Figure 4 shows the bifurcation diagram for the logistic system (left diagram), the Lyapunov exponent λ (middle diag.) and the information entropy $H(\varepsilon)$ (right diag.), with common abscissas of parameter a ($2.8 \leq a \leq 4.0$). It is clear that the bifurcation diagram (left diagram) is quantified by the Lyapunov exponent (middle diag.: not chaos in $\lambda \leq 0$; chaos
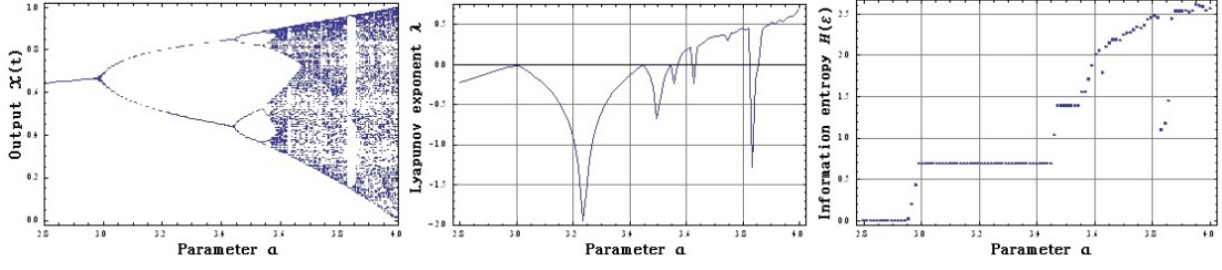
Figure 4. The bifurcation diagram of the logistic map (left diagram) over the parameter range $2.8 \leq a \leq 4.0$, the Lyapunov exponent (middle diag.) and the information entropy (right diag.).

in $\lambda > 0$) and by the information entropy varieing with parameter a (right diag., compare with the left diag.).

3.2. Fractal dimension

In this chapter we aim to infer the cosmic system's evolution by the flux density data radiated from cosmic object and measured by the interferometer (of the radio wave). The fractal dimension is useful to study the system with which the data is related. We have a variety of fractal dimensions; the box counting dimension D_0, the information dimension D_1 and the correlation dimension D_2 as defined in the following equations [see Fig. 5.].
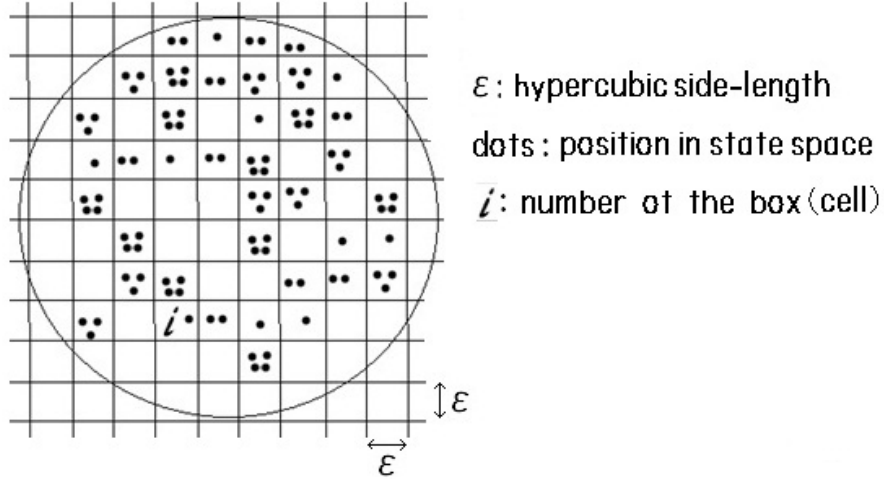

ε : hypercubic side–length

dots : position in state space

i : number of the box (cell)

Figure 5. Diagram of a point distribution in a state space for computing the fractal dimension.

$$D_0 = \lim_{\varepsilon \to 0} \frac{\log M(\varepsilon)}{-\log \varepsilon} \,, D_1 = \lim_{\varepsilon \to 0} \frac{H(\varepsilon)}{-\log \varepsilon} \,, \; D_2 = \lim_{\varepsilon \to 0} \frac{\log \sum_{i=1}^{M} p_i^2}{\log \varepsilon} \tag{4}$$

The fractal dimensions in Eq.(4) are derived from the generalized dimension D_q:

$$D_q = \lim_{\varepsilon \to 0} \frac{1}{q-1} \frac{\log \sum_{i=1}^{M} p_i^q}{\log \varepsilon} \tag{5}$$

for $q = 0$ (the box counting dimension), $q = 1$ (the information dimension at $q \to 1$) and $q = 2$ (the correlation dimension) [1]. It is not easy to compute the fractal dimension from

measured data, even if it is at $q = 0$, because we know little about the system's dynamics, on which we are to study, and in addition, it is impossible to box-count a manifold constructed in a state space with unknown dimension. Fortunately, we have Grassbergar-Procaccia algorithm (GPA) to compute the measured data and substitute the result for the fractal dimension at $q = 2$ [2]. The GPA is discussed in section 5.

4. Dynamical system and time series data

The purpose of this section is to discuss on the problem: if we measure the time series data from a system of nature how we access to a function of the system with which the data is generated. If the nature was constructed by the mathematics it would have been going well to solve the problem. Unfortunately, the nature, I believe, do not go so easy. We need to solve it by devising the data reconstruction and by applying above nonlinear methods to it .

4.1. Time series data

The originally measured data is defined as follows: A measurement starts at time t_0 with sampling rate τ and the time series is expressed in the following way, with i natural number

$$y(t_0), y(t_0 + \tau), \cdots, y(t_0 + i\tau), \cdots$$

If we find a time lag τ' proper for the system in three dimensional state space, the time series is reconstructed, for example, to three dimensional vector $\mathbf{V}_t$ at time t.

$$V_t = (y(t), y(t + \tau'), y(t + 2\tau')); \ t = 1,2, \cdots$$

Vector $\boldsymbol{V}_t$ is embedded in three dimensional time-lagged state space. As the time goes by, the vector draws a trajectory in the state space. The measured data may geometrically express its functional property in this way. The method can be considered to differentiate the data in the state space in a graphycal way. The dimension of the system is unknown in advance, so an original dimension of the reconstructed vector must be searched by changing it one by one until to find the optimal one which is called the embedding dimension. The dynamics of the observed system have a fractal dimension in the embedding dimension. A manifold is drawn in the embedding dimension in this way from the ofserved data and it is called the attractor of the system given by the observed data. From the manifold we infer the original function, as a mathematical nonlinear equation.

4.2. Embedding theory

The attractor is the manifold of a dynamical system, from which a physical quantity is continuausly released to be observed and the time series is, as a result, accessed to be analized. The time series is reconstructed in the form of a vector V_t at m-th dimension to be embedded in the state space. In the following equation the time lag τ' was replaced by τ.

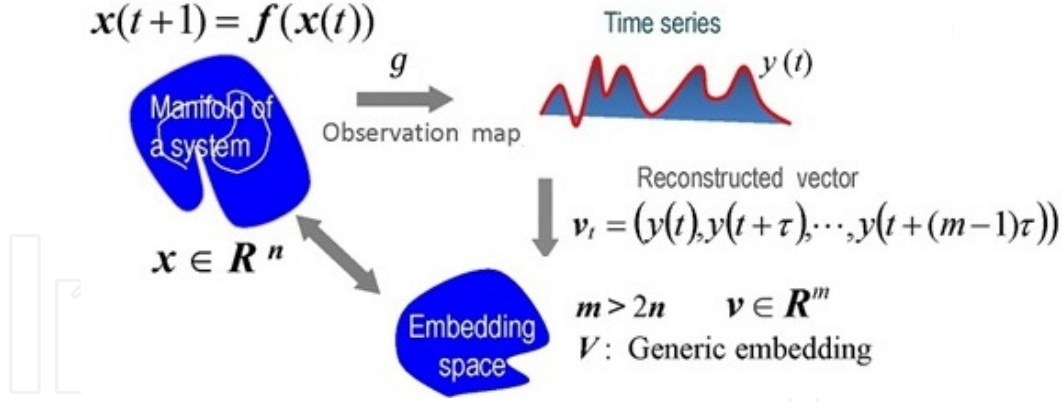$$V_t = (y(t), y(t + \tau), \cdots, y(t + (m - 1)\tau)) \tag{6}$$

Figure 6. Takens' theorem given by a schematic diagram to infer the system's dynamics from measured time series[2].

The data set $\{y(t)\}_{t=t_0}^{t_N}$ is measured by gM, with g the observation map and M the manifold of the system's (source) dynamics at n-th dimension. Takens' theory claims that the attractor reconstructed on the embedding space in Fig. 6 is generic embedding under condition $m > 2n$.[2] The attractor in the embedding state space is a theoretical reflection of the manifold, that is, the embedding map is $V: M \rightarrow R^m$, in which the condition does not need to be satisfied. The source dynamics at the observed system could be inferred in this way. It is generally impossible to solve the function, in a definitive form, of the system's dynamics.

Takens' theorem is summarized in Eq. (7) ~ Eq. (9). h is a map function transforming the embedded attractor into the original attractor.

$$f: M \rightarrow M \quad \Rightarrow \quad g: M \rightarrow R \quad \Rightarrow \quad V: M \rightarrow R^m \tag{7}$$

$$V(x) = \left(g(x), g(f(x)), \cdots, g(f^{m-1}(x))\right) \tag{8}$$

$$h: V \rightarrow M \tag{9}$$

The experimantal expression of Eq.(6), reconstructed by using measured data, corresponds to the theoretical expression of Eq.(8), assuming that a time delay is neglected and the time span is same between both systems. We have the attractor V by analyzing measured data, but it is difficult to have a deterministic expression of the manifold M in Eq.(9).

It is same to say that Galileo Galilei could find experimentally the gravity on the earth, but could not express it in a deterministic expression as the Newton's equation. The map (h) in Eq.(9) is similar to the gravity in the era. At present, it is only possible to get access to the geometrical manifold with the way given in this section. A discussion on the method how to apply the fractal dimension to quantify the geometrical manifold will be given.

It is useful to give attention to noise inevitaby coming into the dynamical system and the observation system. The noise comes into the two systems[2],

$$x(t + 1) = f(x(t)) + \eta(t) \tag{10}$$

$$y(t) = g(x(t)) + \xi(t) \tag{11}$$

where $\eta(t)$ and $\xi(t)$ are system's noise and observation noise, respectively. This makes it very difficult to judge observed data that system's function f is a genuine chaos or not, even if the analysis gives a chaotic result, because the chaos trajectory depends severely on the initial condition.

4.3. Correlation dimension

The attractor is reconstructed in the embedded state space from observed time series. We are interested in the dynamical system of the quasar, the galactic object distributed at cosmological distances (up to ten billions of light years), which releases vast energy by synchrotron radiation and enables us to research some cosmic information by the fluctuations of the microwave flux density. We study the dynamics involving in the time series to know the structure of the dynamics for the system at different cosmological distances. We may be to have some dynamical knowledge of the systems's evolution in the experimental method. The system's information is, in our context, is the manifold for the dynamics of the quasar system at different cosmological distances. The data is the time series of the flux density of the microwaves, 2.7GHz and 8.1GHz, for more than twenty quasars, daily monitored over thousand days. The fractal dimension of the manifold is to be analyzed. The dimensions introduced in the section 3 are difficult to compute with the reconstructed data. Fortunately we have an useful method to compute the correlation dimension developed by Grassberger and Procaccia (GPA) as the substitute of D_2. The algorithm for calculation are the correlation sum and the fractal exponent in the following expressions, N the number of points in the embedding state space at m-th dimension.

Given each point j, k $(j \neq k)$ in Fig. 5 (not number of the cell), with N the number of full points and r the diameter of hypersphere, the correlation sum is expressed by [1,2]

$$C^{(m)}(r) = \frac{1}{N} \sum_{k=1}^{N} \frac{1}{N-1} \sum_{j=1}^{N-1} \theta[r - \|v(j) - v(k)\|], \tag{12}$$

in which $\theta[\cdot]$ is the Heaviside function, counting a pair of m-th dimensional vector points whose distance is within r over all pairs of points. Eq.(12) counts the probability that any pair of state space points meets within a length of r in m-th dimensional state space. The fractal dimension at m-th dimensional state space is expressed by (see Eq.(4))

$$D_2^{(m)} = \lim_{r \to 0} \frac{\log C^{(m)}(r)}{\log r} \tag{13}$$

The optimal correlation dimension D_2 for the attractor embedded in the optimal state space for the time series in question is defined as $D_2^{(m)}$ at $m = m_s$ when the value of $D_2^{(m)}$ ceases to increase as the increase of m. This means that at a full embedding dimension, any points in state space of the attractor can not occupy same position by the no-intersection theorem of chaos [1]. The D_2 is a fractional dimension and the m_s is the embedding dimension in which the system works $(m_s - 1 < D_2 < m_s)$.

4.4. Other methods of analysis

We introduce briefly three methods of analyzing the characteristics of the flux density variation, in which the same data were also computed for reference. The results will cover different aspects of the variation. The first is the spectral index α : The modulus of the fourier spectrum $|A|$, the intensity of the fluctuations at frequency f is computed over the period of 1024 days; the method of least squares was used for the pairs of the logarithms of $|A|$ and f in the frequency range of $\frac{1}{100} \leq f \leq \frac{1}{10}\frac{1}{day}$ to eliminate the major error outside the frequency range. The power law $|A| \propto f^{-\alpha}$ was computed for all of the observed data. The second is the Higuchi's fractal dimension D [9]. The absolute change of the flux density at interval k averaged over the period (1024 days) is computed. Given the averaged change L, the relationship $L \propto k^D$ stands for the interval $1 \leq k \leq 100$ days. The detailed algorithm can be reffered in reference [9]. The dimension D expresses a complexity of the variation in the range $1 \leq D \leq 2$, that is, from liner, $D = 1$, to the plane, $D = 2$, from fractal dimensional view. The third is the Hurst exponent H [10]. Given the ratio R/σ over the interval τ, with range R a difference from top to bottom levels of the reconstructed time series $Y(t) = \sum_{i=1}^{t}(y(i) - \bar{y})$, $\bar{y}$ and σ the average and the standard deviation of $y(i)$, respectively, in the interval τ. The relationship $R/\sigma \propto (\tau/2)^H$ stands in the range of $10 \leq \tau \leq 1000$ days.

The detailed introductions for the methods be referred in [9-11][2]. The result analyzed in these methods will be shown later. The results computed in above principles are useful for cross-checking the knowledge of the result of source dynamics.

5. Time series data

The extragaractic radio sources generate the time series data of the radio wave flux density for us to observe and to analyze their system's dynamics to see a mechanism how the cosmic object has been evolved in the cosmological age from a dynamic aspect of view.[3]

5.1. Monitored cosmic objects

Compact extragaractic radio sources had been monitored daily by Waltmann et al. at GBI radio wave observatory over 3000 days from 1979 [5,6]. Waltmann et al were kind to send us the data of 46 extragalactic objects, from which 21 QSOs and 7 BL Lacs were selected for analysis. At the beginning we analyzed the data in the methods of the spectral index, of the Higuchi's fractal dimension and of the Hurst exponent. The methods will be explained briefly, and the result was published in [7].

The monitored microwave frequencies were at 2.7 and 8.1GHz; and the red shift (the indicator of cosmological distance) of the monitored objects ranged from 0.15 to 2.22 (from one billion to ten billions of light years). The name of the objects are shown in Table 1 as

---

[2] $1/f$ noise characterized as the power law events in the electronic circuit is in reference [11].

well as the red shifts. In Figure 7, the diagrams of the flux density variation over nine years are shown for several quasars.

0133+476*	0202+319	0224+671	0235+164*	0237-234	0333+321	0336-019
0.860	1.466	0.524	0.851	2.224	1.253	0.852
0420-014	0552+398	0828+493	0851+202*	0923+392	0954+658	1245-197
0.915	2.365	0.548	0.306	0.699	0.368	1.275
1328+254	1328+307	1502+106	1555+001	1611+343	1641+399	1741-038
1.055	0.849	1.833	1.770	1.404	0.595	1.054
1749+096*	1749+701*	1821+107	2134+004	2200+420*	2234+282	2251+158*
0.322	0.760	1.036	1.936	0.070	0.795	0.859
Symbol *	BL Lac (7)	; QSO (21)		;		

Table 1. The Name of the extragalactic objects selected for analysis and the red shift [7,8]. Data used for analysis is of 1024 days (start from 2 Feb.1984 observed on daily basis.
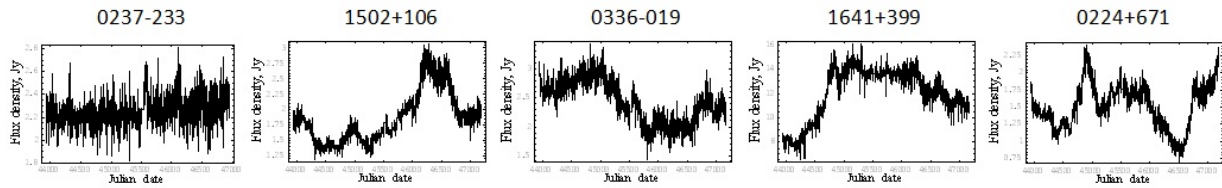

Figure 7. Radio wave flux density variation at 8.1GHz monitored daily over three thousand days. Panels listed in descending order of the magnitude of the red shift. Abscissa: Julian date from 44000 to 47000; ordinate: flux density Jy (10^{-28}W/m^2/Hz) from a few Jy to ten Jy.

5.2. Process of analysis

5.2.1. Correlation dimension

The method of estimating the correlation dimension of the flux density time series of the quasars listed in Table 1 is plainly described here. The correlation sum for the time series data is calculated in the method given in Eq.(12). The time series for the quasar 0224+671, for example, is reconstracted in the way given in subsection 4.2 and embedded in the reconstructed state space (at $m = 3$, for example) as shown at the left diagram (state space diagram) in Fig. 8. The correlation sum is plotted in log scales of abscissa and ordinate according to the diameter r changing its size step by step at each dimension m as shown at the middle diagram in the figure. The correlation exponent is estimeted from the inclination of the correlation sum graph in the way described in Fig. 8. The correlation exponent increase as the increase of the embedding dimension, as shown at the right diagram in Fig. 8, up to the state space dimension to become enough for the original attractor to be contained in the state space. If the exponent stops to increase at an embedding dimension, the exponent, a magnitude less than the embedding dimension, is called the correlation dimension, the fractal dimension, which is thought to reflect the active number of the variables with which the object's system works. It should be taken care that the reliability of the estimated fractal dimension is limited by the number of the data [12]. In our case, the dimension seems to be appropriate values and useful because it will bring cosmological information on the dynamics of object system which is expected to vary with the red shift.
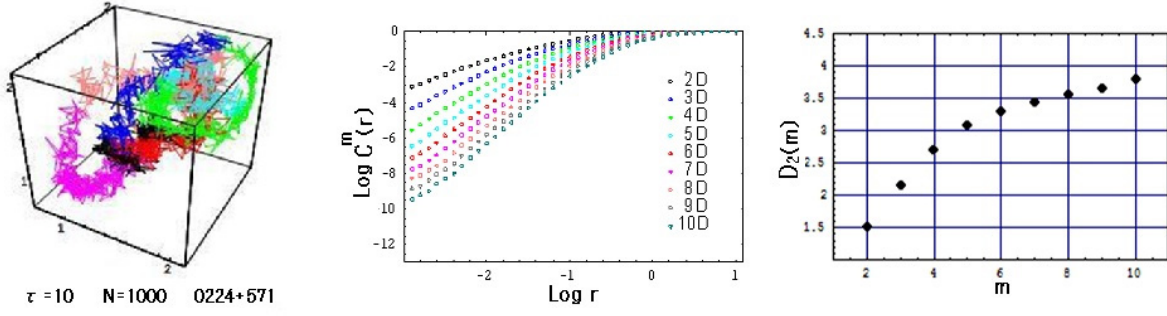
Figure 8. Left diagram: Attractor of the flux density time series for quasar 0224+571 embedded in the reconstructed state space at $m = 3$ ($\tau = 3, N = 1000$), using different colours at time span clarifying the change of state with the passage of time. Middle diagram: Correlation sum computed by using Eq.(12) for each embedding dimension m (parameter from 2 to 10). Right diagram: The correlation exponent was estimated by the inclination of the each curve in the middle diagram at the first order fitting of the least square in the range -3.0<Log r<-1.5. The correlation exponent increases with the increase of the dimension m.

Other indices

A process of analyzing the data with other methods introduced in subsection 4.4 is shown in Fig.9. The diagrams gives us an insight of the way how each index is derived. We will show all of the result analyzed in these methods for a cross reference with the correlation dimension.
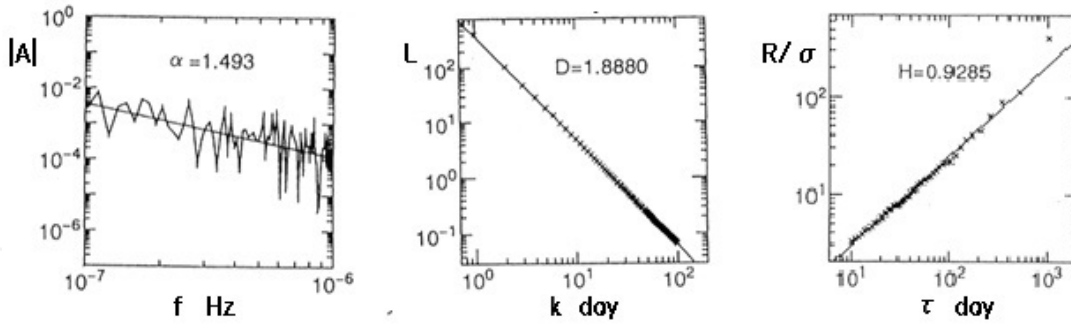

Figure 9. A computing process of analyzing other indices as an example for the time series of the radio wave at 8.1GHz of QSO 1641+399. Left diagram : Spectral index, Middle diagram : Higuchi's fractal dimension, Right diagram : Hurst exponent.

6. Result of analysis

6.1. Correlation dimension

The correlation dimension reflects the dimension of a dynamical function $f(x)$, which is thought to relate closely to the dynamics of monitored radio source. The observation map function g includes the path of radio wave p of the cosmic space and the observation system (antenna) g'; consequently $g = g'p$ stands for the observation map. In Fig.10 we show the

analysis result of the correlation dimension versus the red shift of the object for the data given in Table 1. The result shows a tendency for the both microwaves (2.7 and 8.1GHz) that the correlation dimension increases as the increase of red shift z. It could be said that the complexity of the system's dynamics is increasing as the distance to the quasar is farther. The cosmic spatial map p is unknown for us; on the other hand the data is accessed by $gM = g'pM$, then the system's complexity can be said to depend on the path (map p). In this point, as far as I learned from a radio astronomer at National Astronomical Observatory (Japan), his view was that the influence of p must be weak; if we admit this view, the order in the source dynamics becomes less as the cosmological distance is closer to the Big Bang because the correlation dimension of the system's dynamics can be considered to be a complexity of the system's behavior.
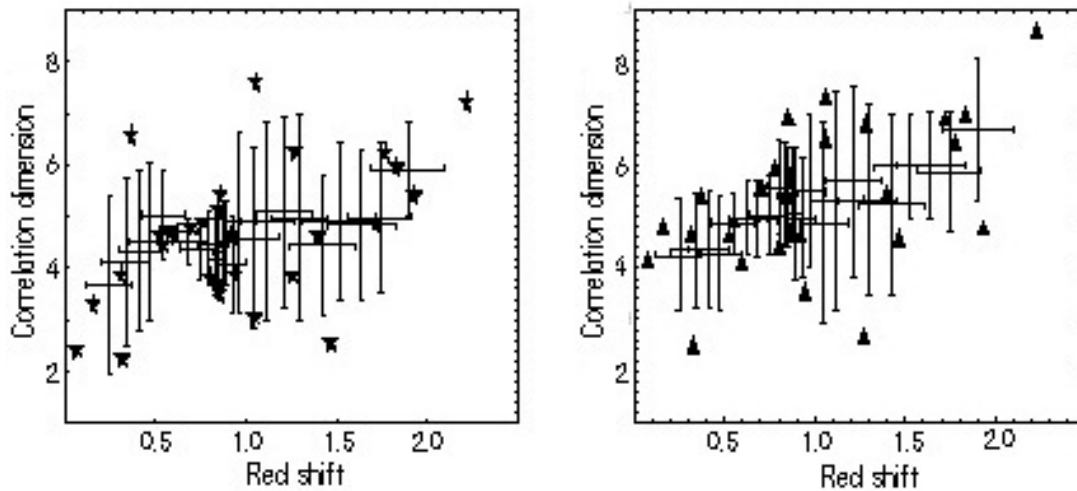

Figure 10. Correlation dimension of the reconstructed attractor for the flux density time series of the quasars given in Table 1 versus the quasar's red shift. Left diagram : 2.7 GH, Right diagram : 8.1 GHz. Horizontal and vertical bars : Running means with error bars at 5 steps along both axes (the red shift and the correlation dimension).

It may be taken care to see the diagram in Fig.10 that the radio wave frequency (2.7 or 8.1 GHz) from which the correlation dimension was derived is the value on the earth; the frequency at the radio wave source must be modified by the red shift (See Table 2); the second is that the sampling rate (one day on the earth) must be also modified on the quasar by the theory of relativity (See Table 2). [7]

red shift z	0.1	0.5	1.0	1.5	2.0	2.5
$1 + z$	1.1	1.5	2.0	2.5	3.0	3.5
$\sqrt{1 - \beta^2}$	0.99	0.92	0.80	0.68	0.60	0.52

Table 2. The Doppler and the relativistic effects. The radio wave frequency is multiplied by $1 + z$ on a quasar at z and the sampling rate on it is multiplied by $\sqrt{1 - \beta^2}$, where β is the ratio of the recession velocity to light velocity.
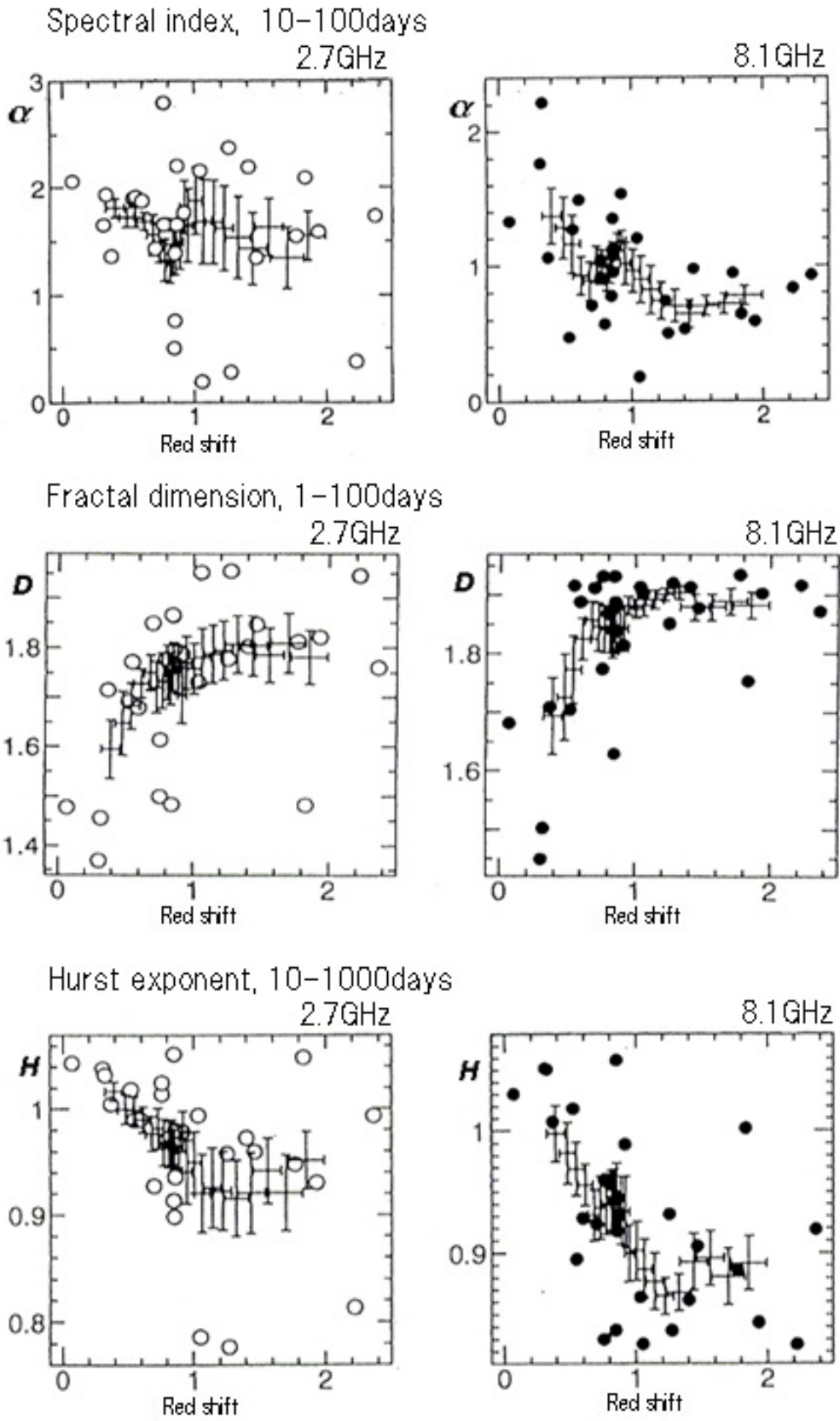
Figure 11. The indices of the flux density time series versus the red shift [7].

6.2. Other indices

Figure 12 shows the result of the indices analyzed in the methods introduced in subsections 4.4 and subsubsection 5.2.2: the diagrams of the spectral index α, the Higuchi's fractal dimension D and the Hurst exponent H versus the red shift z with the holizontal and vertical error bars by calculating the running means over seven points. It may be clear that the indices, α, D and H, vary according to the increase of the red shift in the manner not inconsistent with the correlation dimension D_2 versus z (see Fig. 10). It must be taken in consideration that the indices have their each reflection to the characteristic period due to the algorithm of analysis. It is interesting to see in the graphs of the indices that a typical discontinuity is present at red shift close to $z \approx 1$ (α, H) and the indices do not vary beyond red shift 1.2, $z > 1.2$ (α, D, H). The indices relate to the complexity of how the flux density varies with time; the complexity, α in the frequency domain, D in the fractal dimension of the graph for the density variation and H in the trend persistency. It is useful for us in the empirical way to see the relationship among three indices in our case (see Fig. 12). It may be interesting to see that the relationship between H and D has a systematic dependence despite of the different period concerned, in which the index is based, ten times as much (see Fig.12).
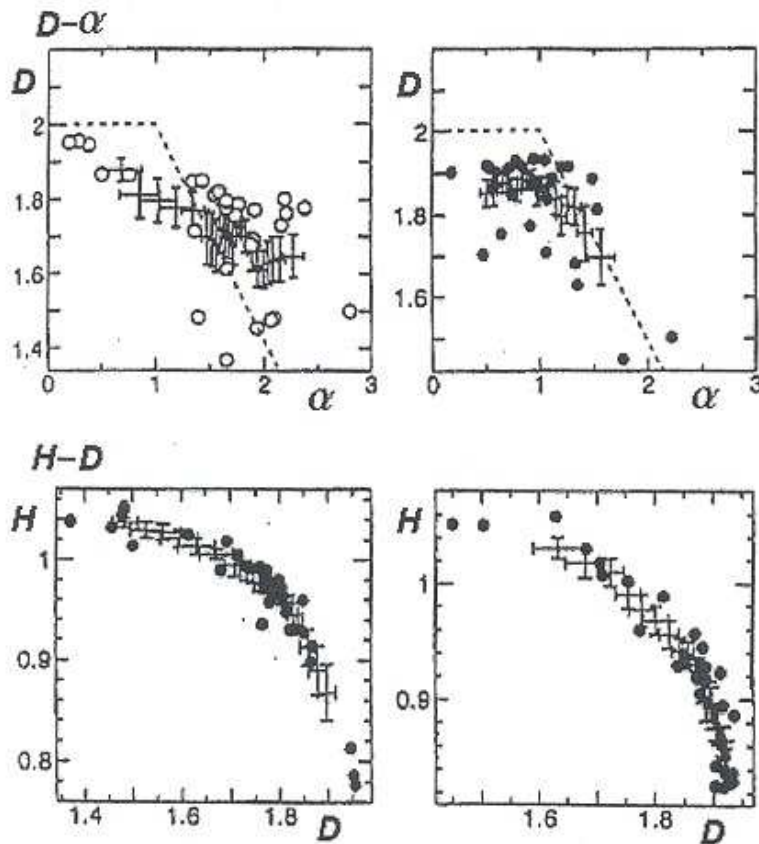

Figure 12. The relationship between the indices D and α (top), and between the indices H and D (bottom) for the 2.7 GHz (left column) and the 8.1 GHz (right column) [7].

6.3. Incident angles of the radio wave to the solar system and to our galaxy

It is natural to have a question that the radio wave flux may be strongly scattered by the matters whose density may be high around the earth (our solar system) and our galaxy; if it is true, there may be a possibility that the indices may affected by the insident angles to our solar system and to our galaxy. The distributions the index D versus right ascension, vs. declination, vs. galactic longitude and vs. galactic latitude are shown in Fig. 13 and Fig. 14. The distributions of the indices other than D may be inferred from the relationships given in Fig. 12. As shown at the bottom ranks in Fig. 13 and Fig. 14, the distribution of the red shift versus the insident angles is almost the same as the distribution of the index versus the insident angles. This became clear from the view in the moving average as give above. We infer that the flux density variation may not be caused by the matters around the earth (our solar system) nor our galaxy, but by any factors related with the red shift (the radio wave path as long as the cosmological distances) and by the system of the radio wave source, the quasar.[13]
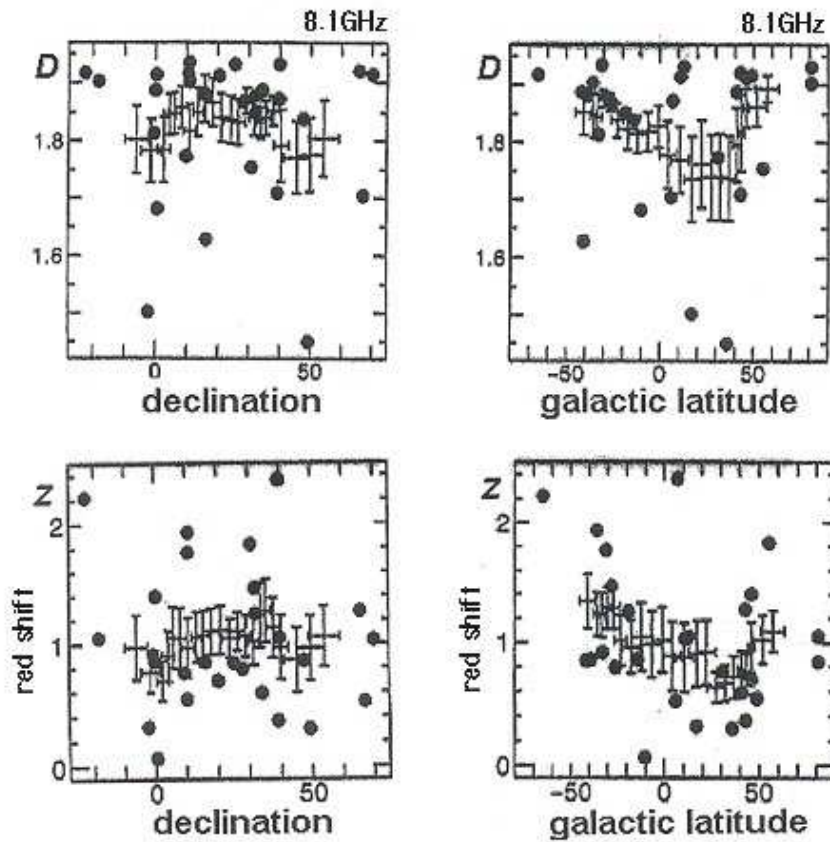

Figure 13. The distribution of the fractal dimension D versus the declination (top, left) and vs. the galactic latitude (top, right) for the radio wave at 8.1GHz, and the distribution of the red shift versus the declination (bottom, left) and vs. the galactic latitude (bottom, right). The vertical and horizontal error bars are of the running means for the numerical values computed by every seven steps. [7]
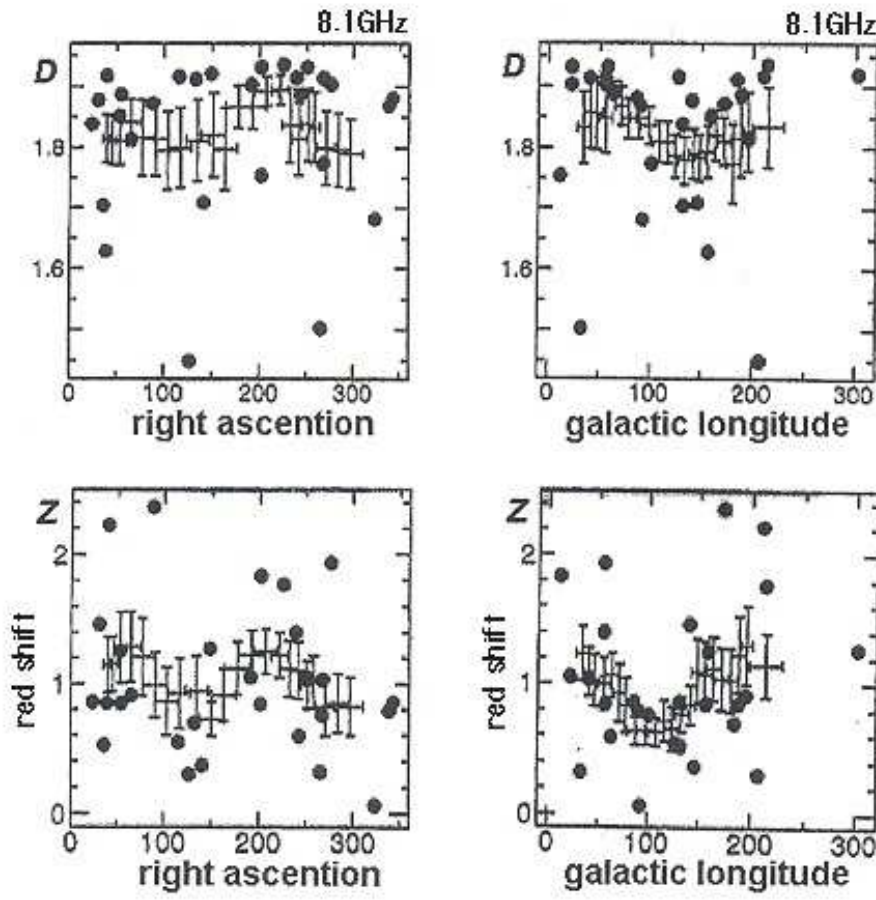
Figure 14. The distribution of the fractal dimension D versus the right ascension (top, left) and vs. the galactic longitude (top, right) for the radio wave at 8.1GHz , and the distribution of the red shift versus the right ascension (bottom, left) and vs. the galactic longitude (bottom, right). The vertical and horizontal error bars are of the running means computed by every seven steps.[7]

7. Conclusion

The correlation dimension D_2 of the flux density variation of the quasar radio wave increases, on average, with the increase in the red shift of quasar up to $z \approx 1$ and reaches a limit at $z \approx 1$, and the dimension depends mainly on the red shift and seems to be not affected, on average, by the incident angles to the earth and to our galaxy, from the view based on our analysis. The result is important because the numerical value of the correlation dimension includes the dynamical dimension of the flux density variation monitored over a thousand days, which reflects a source dynamics as considered in the theory given in section 4 and the dependence on the red shift does not conflict with the dependency of other indices, though we have not yet the knowledge of the external modulation, or the map p, transfering the source dynamics to the antenna. We could not help using such task because of the limitation of the data monitored unintended for our analysis. A systematic and designed observation will be needed to collect data for our analysis. If the analysis will be possible to make based on the purposed data, we will have more reliable reflection of the

system's dynamics, $v_{t+1} = f_z(v_t)$, where f_z is the function at red shift z, in a form of the manifold but not of the equation, and infer a more exact view of the cosmological evolution.

For readers from different fields the literature on the radio galaxies and quasars may be referred in reference[3].

As discussed in section 2., the nonlinear dynamics is sensitive to the initial condition and the parameter. Our hope is to infer a definite dynamical function f_z at red sfift z. The difficulty comes from the following notion due to noise inevitable in the actual system; $\eta(t)$: noise added to the genuin dynamics, and $\xi(t)$: noise added to the observation system;[2]

$$x(t+1) = f_z(x(t)) + \eta(t) \tag{14}$$

$$y(t) = g(x(t)) + \xi(t) \tag{15}$$

We may need to take in mind that our accessed data might have added by noise of Eq.(15) and the analyzed attractor (a reflection of f_z) might have been added by noise of Eq.(14). After all a more complicated process might have been taken into account to estimate our result and study on the evolution of cosmic system.

Author details

Noboru Tanizuka
Complex Systems Laboratory, Tondabayashi, Japan

Acknowledgement

8. References

[1]   Hilborn RC. Chaos and Nonlinear Dynamics. Oxford: Oxford Univ. Press; 2000.

[2]   Aihara K. Fundamentals and Applications for Chaos Time Series Analysis. Tokyo: Sangyo Tosho; 2000.

[3]   Kellermann KI., Owen FN. Radio Galaxies and Quasars. In: Verschuur GL., Kellermann KI. (eds.) Galactic and Extragalactic Radio Astronomy. New York: Springer-Verlag; 1988, p563-602.

[4]   Akabane K., Kaifu N., Tahara H. Cosmic Radio Astronomy. Tokyo: Kyoritsu; 1988.

[5]   Waltmann EB., Fiedler RL., Johnston KJ., Spencer JH.,Florkowski DR., Josties FJ., McCarthy DD., Matsakis DN. Daily Observations of Compact Radio Sources at 2.7 and 8.1GHz: 1979-1987. Astrophys. J. Suppl. Ser. 1991;77(Nov) 379-404.

[6] http://www.gb.nrao.edu/fgdocs/gbi/gbint.html (accessed 14 May 2012)

[7] Tanizuka N., Takano M. Observational Study on a Process of Evolution of Galaxies. IEE J Trans. C 2000;120-C(8/9) 1149-1156.

[8] Tanizuka N., Khan MR. Knowledge from the Time Series of Quasar Radio-Wave Flux Density. Systems and Computers in Japan 2003; 34(10) 56-62.

[9] Higuchi T. Approach to an irregular time series on the basis of the fractal theory. Physica 1988; 31 (D)277-283.

[10] Feder J. Fractals. New York: Plenum; 1989.

[11] Gupta MS., editor. Electrical Noise: Fundamentals & Sources. New York: IEEE Press; 1977.

[12] Ruelle D. Deterministic Chaos: The Science and the Fiction. Proc. R. Soc. London 1990; 427 A: 241-248.

[13] Tanizuka N. Analysis of Quasar Radio Wave Flux Density Fluctuations and its Cosmological Meanings. In Macucci M, Basso G. (eds) Noise and Fluctuations, 20th International Conference on Noise and Fluctuations, ICNF2009, 14-19 June 2009, Pisa, Italy. Melville, New York, AIP Conference Proceedings 1129: 2009 .